Letter

Radiative decay and electromagnetic moments in ^{229}Th determined within nuclear density functional theory

A. Restrepo-Giraldo,[1] J. Dobaczewski,[1,2] J. Bonnard,[1] and X. Sun[1]

[1]*School of Physics, Engineering and Technology, University of York, Heslington, York YO10 5DD, United Kingdom*

[2]*Institute of Theoretical Physics, Faculty of Physics, University of Warsaw, Ulica Pasteura 5, PL-02-093 Warsaw, Poland*

(Received 16 February 2026; accepted 22 October 2026; published 16 November 2026)

Using the nuclear DFT approach with symmetry breaking and restoration, we investigate the electromagnetic properties of the ground and isomeric states in ^{229}Th. We determine the magnetic dipole transition strength $B(M1; 3/2_1^+ \to 5/2_1^+)$ between these two states along with their corresponding spectroscopic magnetic dipole, electric quadrupole, and magnetic octupole moments. We discuss the effects of parity breaking, configuration mixing, and time-odd core polarization. Because the octupole deformability of the standard Skyrme functionals varies, we analyze the results using a set of functionals and perform a regression aligned with the measured electric octupole moments of neighboring even-even nuclei. Without dedicated parameter adjustment, the results compare favorably with the experimental data but also indicate the need to systematically adjust the octupole degrees of freedom in future functional parametrizations.

DOI: 10.1103/khzg-vkgr

Introduction. Since the discovery of the nearly degenerate excited and ground states of ^{229}Th 50 years ago, experimental and theoretical communities have made many efforts to understand and characterize this unusual emergent feature. To date, it is the lowest excited state in the entire nuclear chart, making it a distinctive isomer of interest for experiments, theory, and potential technological applications [1–10]. This unusual property also makes it difficult to study, pushing the limits of experimental and theoretical methods.

Its first detection came from the γ spectrum of α-decaying ^{233}U, where an excited state below 100 eV was proposed to explain its decay scheme [11]. Several subsequent spectroscopic studies helped clarify the excited state and further constrained its energy [12–16]. Later, direct detection of internal-conversion electrons enabled more precise characterization of the isomeric state [17]. Since then, alternative production channels and measurement techniques have been developed to accurately determine its observables, including electromagnetic moments [18–24], perform investigations of internal conversion processes in excited electronic configurations [25], and nuclear hyperfine mixing [26,27].

Because the radiative transition energy is low, the electronic environment strongly influences its properties, making lifetime measurements depend on specific experimental setups and requiring corrections to estimate the corresponding vacuum transition rates. The latest results [28] report a transition energy of $E_\gamma = 8.35574(3)$ eV, a half-life in vacuum of $t_{1/2} = 1740(50)$ s, and a corresponding reduced transition probability of $B(M1) = 0.0217(6)$ W.u.$_{M1}$ = $0.0388(12)\,\mu_N^2$,[1] marking a significant improvement in precision compared to previous studies [10,29]. Note that $1\,\text{W.u.}_{M1} = 1.7905\,\mu_N^2$.

Electromagnetic moments have been measured for both the $3/2^+$ isomeric and $5/2^+$ ground states [30–33]. The latest measurements of spectroscopic electric quadrupole moments are $Q(3/2^+) = 1.77(1)$ b and $Q(5/2^+) = 3.11(2)$ b [6]. For the magnetic dipole moments, the latest reports are $\mu(3/2^+) = -0.378(8)\,\mu_N$ and $\mu(5/2^+) = 0.366(6)\,\mu_N$ [34]. The deviation from the Schmidt limits [35] $\mu_{\text{Sch.}}(5/2) = [1.366, -1.913]\,\mu_N$ and $\mu_{\text{Sch.}}(3/2) = [1.148, -1.913]\,\mu_N$ indicates a strong core polarization effect in this isotope. Magnetic octupole moments are yet to be measured in the actinide region, where for $\langle r^2 \rangle = 33.13(3)\,\text{fm}^2$ in ^{229}Th [36], the Schwartz limits [37] are $\Omega_{\text{Sch.}}(5/2) = [-0.543, 0.181]\,\mu_N$ b and $\Omega_{\text{Sch.}}(3/2) = [-0.380, 0.054]\,\mu_N$ b.

Advances in the experimental field have been motivated by prospective technological applications in areas such as chronometry [38–42], γ-ray laser technology [43,44], and satellite-based navigational and chronological geodesy systems [3]. These developments could enable a new generation of ultraprecise techniques that will also advance scientific research [2,5,6]. However, these developments depend on precise control of excitation and deexcitation between the $3/2^+$ state and the $5/2^+$ ground state, where the $M1$ multipolarity exceeds the competing $E2$ multipolarity by about 10^{13} orders of magnitude because of the extremely low transition energy [45]. Recent advances have achieved the first optically controlled laser excitation in doped crystals of Th:CaF_2 and Th:$LiSrAlF_6$, along with new proposals currently under

[1]Uncertainties are calculated from error propagation of the measurements of $t_{1/2}$ and E_γ.

Published by the American Physical Society under the terms of the Creative Commons Attribution 4.0 International license. Further distribution of this work must maintain attribution to the author(s) and the published article's title, journal citation, and DOI.

development, demonstrating that these applications are feasible [28,46–49].

Theoretical efforts to understand and predict the observables of this elusive isomeric transition have been done in the frameworks of phenomenological [45], core-plus-particle [14,16,50–53], and projected shell models [54]. In these approaches, reliance on adjusted parameters, effective charges, or effective g factors was crucial for accurately reproducing observables. Previous parameter-free self-consistent approaches have been implemented without parity breaking, that is, neglecting the octupole deformation [2], time-reversal and signature symmetry breaking, which preclude angular momentum core polarization [2,55], parity and rotational symmetry restoration [2,56], or configuration interaction [2,55,56] to obtain low-energy structure, multipole moments, and transition strengths.

In this Letter, we present the first analysis, based on self-consistent nuclear density functional theory (DFT) without dedicated parameter adjustment, that incorporates all previously missing elements and employs the methodology of Refs. [57,58], which predates the lifetime measurement [28]; see also Refs. [59–61]. We apply the configuration-interaction multireference DFT (MR-DFT) approach with several Skyrme functionals, mixing two sets of paired, octupole-deformed, and symmetry-restored configurations, one for the ground state and the other for the isomer, and estimate the corresponding $B(M1)$ value and electromagnetic moments. A similar configuration-interaction approach has recently been successfully used to calculate two-neutrino double-β decay matrix elements [62].

Method. We conducted a multistep calculation of the ground and isomeric nuclear wave functions of ^{229}Th to determine the magnetic dipole transition strength $B(M1;\ 3/2_1^+ \rightarrow 5/2_1^+)$ and the electromagnetic moments $Q(3/2^+)$, $Q(5/2^+)$, $\mu(3/2^+)$, $\mu(5/2^+)$, $\Omega(3/2^+)$, and $\Omega(5/2^+)$ for several Skyrme functionals with pairing interaction, implemented in the code HFODD [63–65] version 333 k. We used only the parameters adjusted in previous publications; see the Supplemental Material [66]. We took pairing strengths $V_{0,n}$ and $V_{0,p}$, which reproduce the mass staggering around ^{229}Th and ^{227}Ac, respectively, from Ref. [9]. We took the Landau isovector parameters g_0', which constrain the isovector spin-spin coupling constants to reproduce magnetic dipole moments of doubly magic neighbors or β-decay rates, from Refs. [57,67].

We present results using seven Skyrme functionals: SkX$_c$ [68], SkM* [69], UNEDF1 [70], SIII [71], SkO′ [72], SLy4 [73], and UNEDF0 [74]. Since none of these Skyrme functionals were adjusted to data on octupole degrees of freedom, we anticipated systematic disagreement among the calculations. Therefore, following Ref. [75], we analyzed correlations between the calculated intrinsic octupole moments Q_0^3 and the predicted $B(M1)$ and electromagnetic moments, using the experimental values of Q_0^3 as reference points. To this end, we computed the ground-state octupole moments of ^{226}Ra and ^{230}Th and used the experimental values[2] for these isotopes, $Q_0^3(^{226}\text{Ra}) = 1080(30)$ e fm^3 [76,77] and $Q_0^3(^{230}\text{Th}) = 800(40)$ e fm^3 [78].

Our computational approach blocked specific odd-neutron axial quasiparticle configurations in ^{229}Th and relaxed parity constraints. This yielded deformed, symmetry-breaking solutions with nonzero intrinsic octupole moments Q_0^3. We then projected these solutions onto good parity and angular momentum, forming a mixed wave function.

As discussed in Ref. [61] and in references cited therein, the DFT magnetic moments critically depend on the so-called time-odd (TO) terms of the mean field [79–82], which are solely responsible for the angular momentum polarization of the core. To assess their role in determining the M1 transition rates, we performed all calculations in two variants: (i) with the time-even (TE) terms only and (ii) with both TE and TO terms included. In addition, the TE + TO results were obtained for the isovector spin-spin terms of the functionals, with consistent Landau parameters [67,83] either adjusted to experimental magnetic moments [57] or to the Gamow-Teller strengths [67]; see the Supplemental Material [66].

Procedure. Here, we describe the multistep process used to determine the results of this study. First, for each Skyrme functional, we determined the axial-parity-breaking paired ground-state wave functions of the neighboring even-even isotope ^{228}Th, from which we obtained the corresponding single-particle (s.p.) wave functions. Then, for each of the angular momentum projections along the axis of axial symmetry, $\Omega = 5/2$ and $\Omega = 3/2$,[3] we selected three of them near the Fermi surface for blocking [84–86] in the odd-N isotope ^{229}Th.

In the second step, we used the ^{228}Th s.p. wave functions as tags to self-consistently determine the quasiparticle configurations in ^{229}Th, as explained in Ref. [59]. To establish a common naming convention for those configurations, we use the calculated dominant Nilsson labels[4] of the ^{228}Th tag states, which, following Ref. [60], we denote with parentheses instead of brackets. They are (642)3/2, (741)3/2, and (631)3/2 for $\Omega = 3/2$ and (633)5/2, (752)5/2, and (622)5/2 for $\Omega = 5/2$. We also consider parity-broken configurations with Nilsson labels $N_0 = 7$, as they may acquire positive-parity components after parity restoration.

The tagging technology enables tracking of blocked quasiparticle states throughout the self-consistent iterations, regardless of their changing energies and deformations. In this way, we obtained the self-consistent symmetry-broken ^{229}Th wave functions $|\Phi_{n\Omega}\rangle$ for the three lowest configurations, $n = 1$, 2, and 3, of $\Omega = 5/2$ and $\Omega = 3/2$. In some cases, the Nilsson labels of the blocked self-consistent quasiparticle orbitals can differ from those of the tag states, which may occur when a given Nilsson state $[N_0 n_z \Lambda]\Omega$ is not strongly dominant, as discussed in Ref. [61].

[2]We use the same convention for Q_0^3 as in Ref. [75].

[3]We are bound to keep the traditional notation, denoting by the same symbol Ω both the projections of the angular momentum on the axis of axial symmetry and the magnetic octupole moment.

[4]The dominant Nilsson labels [87] correspond to the largest component of a given s.p. state when it is expanded on the asymptotic Nilsson states $[N_0 n_z \Lambda]\Omega$ [84].

Then, in the third step, we restored broken symmetries [88] by projecting wave functions $|\Phi_{n\Omega}\rangle$ onto good angular momentum I and positive parity $\pi = +$. We denote the resulting band-head wave functions ($I = |\Omega|$) as $|\Phi_{nI^+\Omega}\rangle$, that is, $|\Phi_{n5/2^+5/2}\rangle$ and $|\Phi_{n3/2^+3/2}\rangle$. Previous tests have shown [59] that particle-number restoration does not affect magnetic moments. Because it increases computation time by 2 orders of magnitude, we did not perform it in this study.

In the fourth step, for $I^\pi = 5/2^+$ and $I^\pi = 3/2^+$, we solved two configuration-interaction equations (the Hill-Wheeler equations [81,84]),

$$\sum_{n'} H^{I^+\Omega}_{nn'} a_{n'I^+\Omega} = E \sum_{n'} N^{I^+\Omega}_{nn'} a_{n'I^+\Omega}, \tag{1}$$

where two sets of 3×3 matrix elements of the Hamiltonian $H^{I^+\Omega}_{nn'}$ and overlap $N^{I^+\Omega}_{nn'}$ read as follows,

$$H^{I^+\Omega}_{nn'} = \langle \Phi_{nI^+\Omega} | \hat{H} | \Phi_{n'I^+\Omega} \rangle, \tag{2}$$

$$N^{I^+\Omega}_{nn'} = \langle \Phi_{nI^+\Omega} | \Phi_{n'I^+\Omega} \rangle, \tag{3}$$

for $I = \Omega = 5/2$ and $I = \Omega = 3/2$. We calculated the Hamiltonian matrix elements (2) using the standard methodology defined in the generator coordinate method for Skyrme functionals [81,84]. For both sets, we considered only the lowest-energy solutions E, corresponding to mixing coefficients $a_{n'I^+\Omega}$ and normalized mixed wave functions,

$$|\Phi_{I^+\Omega}\rangle = \sum_n a_{nI^+\Omega} |\Phi_{nI^+\Omega}\rangle. \tag{4}$$

We note that the states $|\Phi_{n'I^+\Omega}\rangle$ are generally nonorthogonal ($N^{I^+\Omega}_{nn'} \neq \delta_{nn'}$); therefore, the mixing coefficients $a_{n'I^+\Omega}$ cannot be interpreted as probability amplitudes.

In the fifth step, we calculated the set of 6×6 matrix elements of the magnetic dipole $\hat{M}$, the electric quadrupole $\hat{Q}$, and the magnetic octupole $\hat{\Omega}$,

$$O^{II'}_{nn'} = \langle \Phi_{nI^+I} | \hat{O} | \Phi_{n'I'^+I'} \rangle, \tag{5}$$

where $\hat{O}$ represents operator $\hat{M}$, $\hat{Q}$, or $\hat{\Omega}$.

In the final sixth step, we could then determine the MR-DFT matrix element of the $M1$ transition between the $I^\pi = 5/2^+$ and $I^\pi = 3/2^+$ states,

$$\langle \Phi_{5/2^+5/2} | \hat{M} | \Phi_{3/2^+3/2} \rangle = \sum_{nn'} a^*_{n5/2^+5/2} M^{\frac{5}{2}\frac{3}{2}}_{nn'} a_{n'3/2^+3/2}, \tag{6}$$

and the corresponding reduced transition probability,

$$B(M1; 3/2^+_1 \to 5/2^+_1) = \tfrac{1}{4} |\langle \Phi_{5/2^+5/2} | \hat{M} | \Phi_{3/2^+3/2} \rangle|^2. \tag{7}$$

Similarly, we determined the spectroscopic magnetic dipole, electric quadrupole, and magnetic octupole moments of the $I^\pi = 5/2^+$ and $I^\pi = 3/2^+$ states as follows,

$$\langle \Phi_{I^+I} | \hat{O} | \Phi_{I^+I} \rangle = \sum_{nn'} a^*_{nI^+I} O^{II}_{nn'} a_{n'I^+I}. \tag{8}$$

Our approach does not explicitly rely on collective gyromagnetic factors, since such effects arise naturally from core polarization and symmetry restoration [60]. Moreover, we set the orbital and spin gyromagnetic factors in the magnetic-operator definitions to their free-nucleon values, as in Ref. [57].

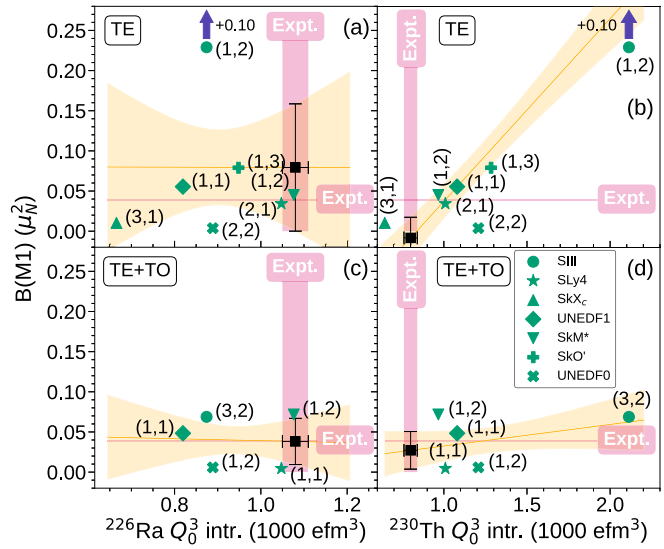


FIG. 1. $B(M1)$ values of the ^{229}Th isomer decay with respect to the intrinsic octupole moments Q_0^3 of ^{226}Ra [panels (a) and (c)] and ^{230}Th [panels (b) and (d)], determined for functionals reduced to the time-even mean fields [TE, panels (a) and (b)] and with complete time-even and time-odd mean fields [TE + TO, panels (c) and (d)]. The numbers in parentheses indicate the numbers of successfully mixed wave functions for the two configurations, namely ($5/2^+$, $3/2^+$). Vertical and horizontal stripes labeled Expt. are the experimental values of Q_0^3 and $B(M1)$, respectively. Thick lines and shaded bands denote the regression results and their uncertainties, respectively [75]. Arrows denote points shifted outside the figure's scale.

We also note that describing the smallness of the isomeric energy in ^{229}Th is most likely beyond the reach of any nuclear theory and certainly beyond the capability of nuclear DFT. In our opinion, this smallness is not due to any symmetry or physical property of the system but is simply an accident. Therefore, we focus on electromagnetic observables that characterize the intrinsic structure of both states.

As shown and discussed in Ref. [60], the magnetic properties of interest here are largely independent of detailed energy splitting or orbital ordering near the Fermi level. In that reference, the calculated magnetic dipole moments very weakly depend on quasiparticle energies and deformations across the entire major shell and many MeV of excitation energies. We conclude that the calculated isomeric energies of ^{229}Th, which, on the scale of a few hundred keV, are essentially random across the set of functionals employed, do not affect the wave function's electromagnetic properties, and, in our opinion, are irrelevant to the results presented in this Letter.

In addition, we do not include any triaxiality in our calculation for practical rather than physical reasons, as discussed in Ref. [61]. We fix the wave functions with the correct quantum numbers and single-particle configurations dominated by specific axially symmetric Nilsson states. After restoring rotational and parity symmetries, the transition between the $3/2^+$ and $5/2^+$ configurations is allowed by the $M1$ selection rules, enabling us to determine the matrix-element magnitude and

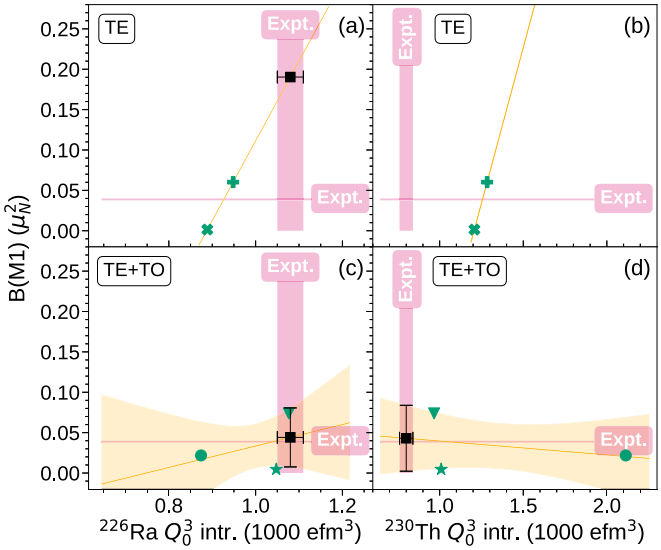


FIG. 2. Same as in Fig. 1 but for the $B(M1)$ values calculated between converged individual (not mixed) blocked self-consistent states [631]3/2 and [633]5/2.

thus $B(M1)$. In this methodology, unlike phenomenological approaches, exact symmetry restoration removes the need to account for Coriolis effects.

Results. Figure 1 presents our study's principal findings. It compares the TE $B(M1)$ values [Figs. 1(a) and 1(b)] with the TE + TO values [Figs. 1(c) and 1(d)] derived from the measured intrinsic octupole moments in ^{226}Ra [Figs. 1(a) and 1(c)] and ^{230}Th [Figs. 1(b) and 1(d)] . In each case, we analyzed results for different Skyrme functionals using the linear regression method of Ref. [75] and extrapolated to the measured points with uncertainties.

Encouragingly, the TE + TO results extrapolated to the experimental data for ^{226}Ra and ^{230}Th are consistent with

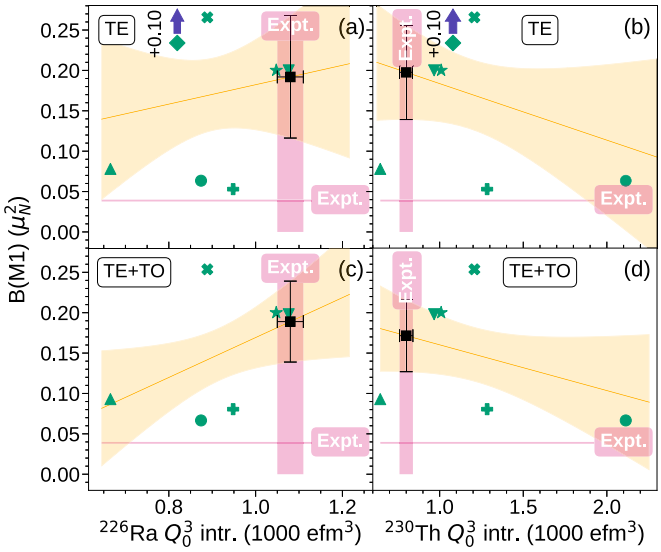


FIG. 3. Same as in Fig. 2 but for the $B(M1)$ values calculated between parity-conserving states.

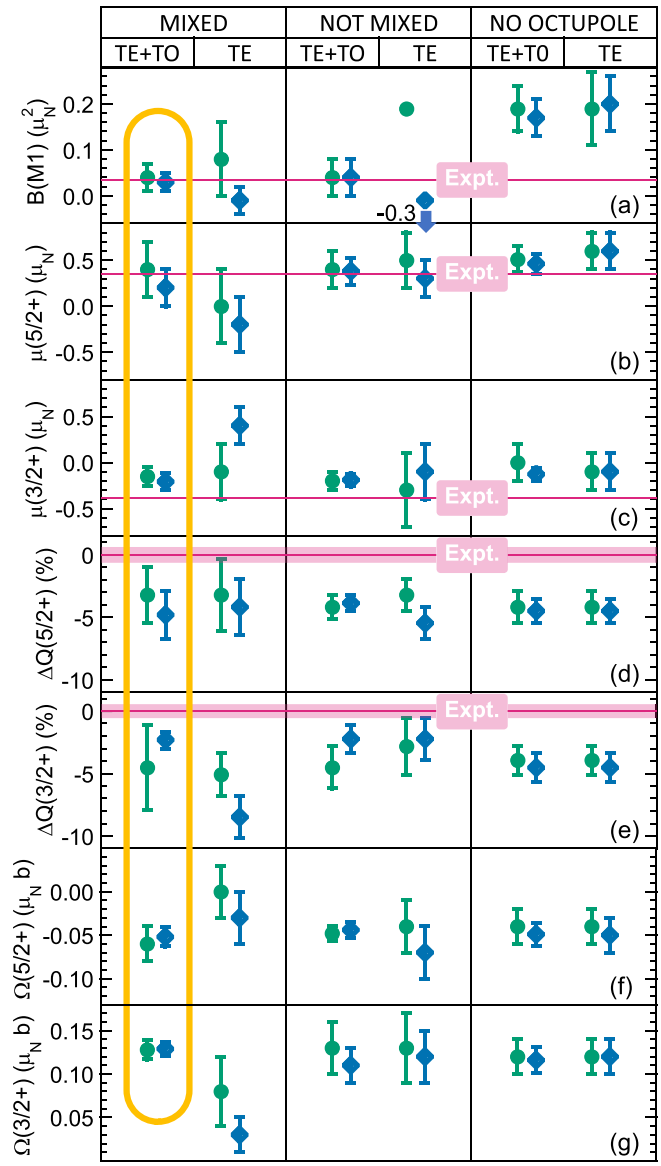


FIG. 4. Summary of results obtained in this Letter, compared with the experimental data [6,28,34]. The shown values are the following: reduced transition probabilities $B(M1)$ (a), magnetic dipole moments μ of the $5/2^+$ (b) and $3/2^+$ (c) states, percentage deviations from the data ΔQ of the electric quadrupole moments of the $5/2^+$ (d) and $3/2^+$ (e) states, and magnetic octupole moments Ω of the $5/2^+$ (f) and $3/2^+$ (g) states. Circles and diamonds correspond to regressions aligned with the measured octupole moments of ^{226}Ra and ^{230}Th, respectively, for the functionals specified in the figures of the Supplemental Material [66], as indicated by the specific case at the top of the current figure.

each other, yielding $B(M1) = 0.04(3)$ and $0.03(2)$ μ_N^2, respectively (uncertainties calculated by the regression method). It is also gratifying that both agree with the experimental value of $0.0388(12)$ μ_N^2 (value and uncertainty calculated from the experimental results [28]). However, the large spread in results from different Skyrme functionals leads to theoretical uncertainties much larger than the experimental uncertainty.

TABLE I. Same as in Fig. 4 but for the weighted averages of the results obtained for the ^{226}Ra and ^{230}Th mixed and TE + TO regressions. The specific functionals involved in each calculation can be inspected from the corresponding figures in the Supplemental Material [66]. Columns Δ and Δ (%) show differences and percentage differences, respectively, between DFT and experiment.

^{229}Th	I_1^π	DFT	Expt.	Δ	Δ (%)
B(M1) (μ_N^2)	$3/2_1^+ \to 5/2_1^+$	0.03(2)	0.0388(12)	−0.006(17)	−20(40)
μ (μ_N)	$5/2_1^+$	0.3(3)	0.366(6)	−0.10(17)	−30(50)
	$3/2_1^+$	−0.18(7)	−0.378(8)	0.19(7)	−50(20)
Q (b)	$5/2_1^+$	2.98(5)	3.11(2)	−0.13(5)	−4(2)
	$3/2_1^+$	1.728(12)	1.77(1)	−0.042(15)	−2.4(9)
Ω (μ_N b)	$5/2_1^+$	−0.054(10)	–	–	–
	$3/2_1^+$	0.129(6)	–	–	–

The TE results, characterized by large outlier SIII values, read $B(M1) = 0.08(8)$ and –0.01(3) μ_N^2, respectively.[5] They are less compatible with experiment, less consistent with one another, and may exhibit greater uncertainty. These results thus indicate the importance of time-odd mean fields in describing the $B(M1)$ value in ^{229}Th.

The main challenge in obtaining the results shown in Fig. 1 is that the Hamiltonian mixing matrix elements $H_{nn'}^{I^+\Omega}$ are often singular due to nonzero self-interaction and self-pairing energies that characterize Skyrme functionals (see discussion in Ref. [88]). This problem remains unresolved, although the search for a solution continues [89–91]. In this work, we removed all singular cases from the analysis (see the Supplemental Material [66]), and the number retained is shown in parentheses in Fig. 1.

As shown in Fig. 2, configuration interaction has a limited effect on the $B(M1)$ values. The figure shows values calculated for only one $3/2^+$ configuration [631]3/2 and one $5/2^+$ configuration [633]5/2. For the TE + TO option, the results are nearly identical to those obtained with the mixed configurations. However, we discarded all points that did not converge properly; see the Supplemental Material [66].

Finally, Fig. 3 presents results obtained by preserving the parity of the [631]3/2 and [633]5/2 states in ^{229}Th. Neglecting octupole deformation yields a significant discrepancy with the experimental $B(M1)$ value and is therefore unacceptable.

Figure 4(a) compares all the $B(M1)$ results discussed above with the experimental value. To benchmark our methods against other experimentally known electromagnetic observables in ^{229}Th, Figs. 4(b)–4(e) summarize results for the magnetic dipole moments, plotted on an absolute scale in Figs. 4(b) and 4(c), and the electric quadrupole moments, plotted on a percentage-deviation scale, $\Delta Q = (Q_{\rm DFT} - Q_{\rm Expt})/Q_{\rm Expt}$, in Figs. 4(d) and 4(e). In Figs. 4(f) and 4(g), we show the DFT predictions for yet-unmeasured magnetic octupole moments.

We observe that the TE + TO moments of both the $5/2^+$ and $3/2^+$ states do not strongly depend on the version of our calculation; however, this is not the case for the mixed magnetic moments obtained by omitting the TO terms. Additionally, results obtained for individual functionals may depend significantly on the inclusion of TO terms; see the Supplemental Material [66]. All results are closest to the data for the most advanced calculation version, marked by the oval in Fig. 4. In Table I, we list the weighted averages of the results determined for the ^{226}Ra and ^{230}Th regressions.

The magnetic moment of the $5/2^+$ ground state is well reproduced, whereas that of the isomer $3/2^+$ is underestimated by about a factor of 2. Nonetheless, this discrepancy does not hinder the accurate replication of the $B(M1)$ value in the oval of Fig. 4(a). The quadrupole moments of both states are reproduced with high accuracy; the calculations agree with the data to within a few percent. The magnetic octupole moments are predicted with relatively small uncertainties. They appear to be weakly affected by differences in the electric octupole moments. The Supplemental Material includes numerical results and plots showing the regression analyses for the electromagnetic moments [66].

Conclusions. We presented the first application of nuclear DFT to the challenging problem of describing the electromagnetic properties of ^{229}Th, including the decay rate of its low-energy isomer. We addressed three fundamental questions in describing these properties: the role of configuration interaction, time-odd core polarization, and octupole correlations within a fully symmetry-conserving approach. Since the isomer and ground-state configurations can be confidently based on two distinct deformed neutron orbitals, the main physics of the problem concerns details of their structure. Our results indicate that configuration interaction is probably small, time-odd polarization is significant, and including octupole correlations is fundamental. We reached these conclusions within a theory that allows symmetry breaking while fully respecting symmetry restoration.

The consistent description of the data obtained without dedicated parameter adjustments is gratifying. Still, the need to properly account for octupole correlations points to the most important way to improve the approach's predictive power: fine-tuning the functional's octupole polarizability through global adjustments to experimental data. Additionally, considering several functionals lets us account for uncertainties in the DFT approach to the model's joint predictions, as reflected in the large error bars, a limitation already described in Ref. [92]. In practice, existing functionals

[5]The negative value (within the error bar compatible with zero) results from linear-regression extrapolation of positive values calculated for different Skyrme functionals.

also have a fundamental drawback: they struggle with self-interactions and self-pairing, making many applications erratic and unacceptable. An intensified effort in these two directions is strongly warranted.

Acknowledgments. We thank Herlik Wibowo for fruitful discussions and Pierre Becker and Alessandro Pastore for their early involvement in the project. COLFUTURO financially supported A.R.-G. This work was partially supported by the STFC, under Grants No. ST/V001035/1 and No. ST/Y000285/1, and by a Leverhulme Trust Research Project Grant. We thank the CSC-IT Center for Science, Ltd., Finland, and the IFT Computer Center at the University of Warsaw, Poland, for allocating computational resources. This project was partly undertaken on the Viking Cluster, a high-performance computing facility provided by the University of York. We are grateful for computational support from the University of York High Performance Computing Service, Viking, and the Research Computing team. We thank Grammarly for its support with English writing.

Data availability. The data that support the findings of this article are openly available [93].

[1] X.-t. He and Z.-z. Ren, Enhanced sensitivity to variation of fundamental constants in the transitions of ^{229}Th and ^{249}Bk, J. Phys. G: Nucl. Part. Phys. **34**, 1611 (2007).

[2] E. Litvinova, H. Feldmeier, J. Dobaczewski, and V. Flambaum, Nuclear structure of lowest ^{229}Th states and time-dependent fundamental constants, Phys. Rev. C **79**, 064303 (2009).

[3] P. G. Thirolf, B. Seiferle, and L. von der Wense, The 229-thorium isomer: Doorway to the road from the atomic clock to the nuclear clock, J. Phys. B: At., Mol. Opt. Phys. **52**, 203001 (2019).

[4] A. Caputo, D. Gazit, H.-W. Hammer, J. Kopp, G. Paz, G. Perez, and K. Springmann, Sensitivity of nuclear clocks to new physics, Phys. Rev. C **112**, L031302 (2025).

[5] E. Fuchs, F. Kirk, E. Madge, C. Paranjape, E. Peik, G. Perez, W. Ratzinger, and J. Tiedau, Searching for dark matter with the ^{229}Th nuclear lineshape from laser spectroscopy, Phys. Rev. X **15**, 021055 (2025).

[6] K. Beeks, G. A. Kazakov, F. Schaden, I. Morawetz, L. Toscani De Col, T. Riebner, M. Bartokos, T. Sikorsky, T. Schumm, C. Zhang, T. Ooi, J. S. Higgins, J. F. Doyle, J. Ye, and M. S. Safronova, Fine-structure constant sensitivity of the Th-229 nuclear clock transition, Nat. Commun. **16**, 9147 (2025).

[7] X.-t. He and Z.-z. Ren, Temporal variation of the fine structure constant and the strong interaction parameter in the ^{229}Th transition, Nucl. Phys. A **806**, 117 (2008).

[8] J. Arakawa, J. F. Doyle, E. Fuchs, J. S. Higgins, F. Kirk, K. Li, T. Ooi, G. Perez, W. Ratzinger, M. S. Safronova, T. Schumm, J. Ye, and C. Zhang, Probing ultralight dark matter at the Mega-Planck scale with the thorium nuclear clock, arXiv:2602.16804.

[9] M. Athanasakis-Kaklamanakis, M. Au, A. Kyuberis, C. Zülch, K. Gaul, H. Wibowo, L. Skripnikov, L. Lalanne, J. R. Reilly, Á. Koszorús, S. Bara, J. Ballof, R. Berger, C. Bernerd, A. Borschevsky, A. A. Breier, K. Chrysalidis, T. E. Cocolios, R. P. de Groote, A. Dorne, *et al.*, Laser spectroscopy and CP-violation sensitivity of actinium monofluoride, Nature (London) **648**, 562 (2025).

[10] X. Lu, R. Zhao, and S.-G. Zhou, The ^{229}Th isomer: Nuclear structure, clocks, and tests of fundamental physics, Chinese Phys. B **35**, 080601 (2026).

[11] L. Kroger and C. Reich, Features of the low-energy level scheme of ^{229}Th as observed in the α-decay of ^{233}U, Nucl. Phys. A **259**, 29 (1976).

[12] R. G. Helmer and C. W. Reich, An excited state of ^{229}Th at 3.5 eV, Phys. Rev. C **49**, 1845 (1994).

[13] E. Peik and C. Tamm, Nuclear laser spectroscopy of the 3.5 eV transition in Th-229, Europhys. Lett. **61**, 181 (2003).

[14] E. Ruchowska, W. A. Płóciennik, J. Żylicz, H. Mach, J. Kvasil, A. Algora, N. Amzal, T. Bäck, M. G. Borge, R. Boutami, P. A. Butler, J. Cederkäll, B. Cederwall, B. Fogelberg, L. M. Fraile, H. O. U. Fynbo, E. Hagebø, P. Hoff, H. Gausemel, A. Jungclaus, *et al.*, Nuclear structure of ^{229}Th, Phys. Rev. C **73**, 044326 (2006).

[15] S. Matinyan, Lasers as a bridge between atomic and nuclear physics, Phys. Rep. **298**, 199 (1998).

[16] K. Gulda, W. Kurcewicz, A. J. Aas, M. J. G. Borge, D. G. Burke, B. Fogelberg, I. S. Grant, E. Hagebø, N. Kaffrell, J. Kvasil, G. Løvhøiden, H. Mach, A. Mackova, T. Martinez, G. Nyman, B. Rubio, J. L. Tain, O. Tengblad, and T. F. Thorsteinsen, The nuclear structure of ^{229}Th, Nucl. Phys. A **703**, 45 (2002).

[17] L. von der Wense, B. Seiferle, M. Laatiaoui, J. B. Neumayr, H.-J. Maier, H.-F. Wirth, C. Mokry, J. Runke, K. Eberhardt, C. E. Düllmann, N. G. Trautmann, and P. G. Thirolf, Direct detection of the ^{229}Th nuclear clock transition, Nature (London) **533**, 47 (2016).

[18] J. Thielking, M. V. Okhapkin, P. Głowacki, D. M. Meier, L. von der Wense, B. Seiferle, C. E. Düllmann, P. G. Thirolf, and E. Peik, Laser spectroscopic characterization of the nuclear-clock isomer ^{229m}Th, Nature (London) **556**, 321 (2018).

[19] D. Moritz, K. Scharl, M. Wiesinger, G. Holthoff, T. Teschler, M. I. Hussain, J. R. Crespo López-Urrutia, T. Dickel, S. Ding, C. E. Düllmann, E. R. Hudson, S. Kraemer, L. Löbell, C. Mokry, J. Runke, B. Seiferle, L. von der Wense, F. Zacherl, and P. G. Thirolf, A cryogenic Paul trap for probing the nuclear isomeric excited state ^{m}Th^{3+}, Eur. Phys. J. D **79**, 127 (2025).

[20] M. Verlinde, S. Kraemer, J. Moens, K. Chrysalidis, J. G. Correia, S. Cottenier, H. De Witte, D. V. Fedorov, V. N. Fedosseev, R. Ferrer, L. M. Fraile, S. Geldhof, C. A. Granados, M. Laatiaoui, T. A. L. Lima, P.-C. Lin, V. Manea, B. A. Marsh, I. Moore, L. M. C. Pereira, *et al.*, Alternative approach to populate and study the ^{229}Th nuclear clock isomer, Phys. Rev. C **100**, 024315 (2019).

[21] S. Kraemer, J. Moens, M. Athanasakis-Kaklamanakis, S. Bara, K. Beeks, P. Chhetri, K. Chrysalidis, A. Claessens, T. E. Cocolios, J. G. M. Correia, H. D. Witte, R. Ferrer, S. Geldhof, R. Heinke, N. Hosseini, M. Huyse, U. Köster, Y. Kudryavtsev, M. Laatiaoui, R. Lica, *et al.*, Observation of the radiative decay of the ^{229}Th nuclear clock isomer, Nature (London) **617**, 706 (2023).

[22] G. Zitzer, J. Tiedau, C. E. Düllmann, M. V. Okhapkin, and E. Peik, Laser spectroscopy on the hyperfine structure and isotope shift of sympathetically cooled ^{229}Th^{3+} ions, Phys. Rev. A **111**, L050802 (2025).

[23] Y.-Y. Xu, Q. Xiao, J.-H. Cheng, W.-Y. Zhang, and T.-P. Yu, Charge-state regulation of nuclear excitation by electron capture in ^{229}Th ions, Nucl. Sci. Tech. **37**, 177 (2026).

[24] S. V. Pineda, P. Chhetri, S. Bara, Y. Elskens, S. Casci, A. N. Alexandrova, M. Au, M. Athanasakis-Kaklamanakis, M. Bartokos, K. Beeks, C. Bernerd, A. Claessens, K. Chrysalidis, T. E. Cocolios, J. G. Correia, H. De Witte, R. Elwell, R. Ferrer, R. Heinke, E. R. Hudson, *et al.*, Radiative decay of the ^{229m}Th nuclear clock isomer in different host materials, Phys. Rev. Res. **7**, 013052 (2025).

[25] P. V. Bilous, G. A. Kazakov, I. D. Moore, T. Schumm, and A. Pálffy, Internal conversion from excited electronic states of ^{229}Th ions, Phys. Rev. A **95**, 032503 (2017).

[26] J. Zhou and X. Wang, Effects of nuclear hyperfine mixing on ^{229}Th^{3+} ions, Phys. Rev. Lett. **136**, 092503 (2026).

[27] V. A. Dzuba and V. V. Flambaum, Shift of nuclear clock transition frequency in ^{229}Th ions due to hyperfine interaction, Phys. Rev. A **108**, 062813 (2023).

[28] J. Tiedau, M. V. Okhapkin, K. Zhang, J. Thielking, G. Zitzer, E. Peik, F. Schaden, T. Pronebner, I. Morawetz, L. T. De Col, F. Schneider, A. Leitner, M. Pressler, G. A. Kazakov, K. Beeks, T. Sikorsky, and T. Schumm, Laser excitation of the Th-229 nucleus, Phys. Rev. Lett. **132**, 182501 (2024).

[29] P. Thirolf, Shedding light on the thorium-229 nuclear clock isomer, Physics **17**, 71 (2024).

[30] S. Gerstenkorn, P. Luc, J. Verges, D. W. Englekemeir, J. E. Gindler, and F. S. Tomkins, Structures hyperfines du spectre d'étincelle, moment magnétique et quadrupolaire de l'isotope ^{229}Th, J. Phys. Fr. **35**, 483 (1974).

[31] C. J. Campbell, A. G. Radnaev, and A. Kuzmich, Wigner crystals of ^{229}Th for optical excitation of the nuclear isomer, Phys. Rev. Lett. **106**, 223001 (2011).

[32] M. S. Safronova, U. I. Safronova, A. G. Radnaev, C. J. Campbell, and A. Kuzmich, Magnetic dipole and electric quadrupole moments of the ^{229}Th nucleus, Phys. Rev. A **88**, 060501(R) (2013).

[33] S. G. Porsev, M. S. Safronova, and M. G. Kozlov, Precision calculation of hyperfine constants for extracting nuclear moments of ^{229}Th, Phys. Rev. Lett. **127**, 253001 (2021).

[34] A. Yamaguchi, Y. Shigekawa, H. Haba, H. Kikunaga, K. Shirasaki, M. Wada, and H. Katori, Laser spectroscopy of triply charged ^{229}Th isomer for a nuclear clock, Nature (London) **629**, 62 (2024).

[35] T. Schmidt, Über die magnetischen momente der atomkerne, Z. Phys. **106**, 358 (1937).

[36] I. Angeli and K. Marinova, Table of experimental nuclear ground state charge radii: An update, At. Data Nucl. Data Tables **99**, 69 (2013).

[37] C. Schwartz, Theory of hyperfine structure, Phys. Rev. **97**, 380 (1955).

[38] C. J. Campbell, A. G. Radnaev, A. Kuzmich, V. A. Dzuba, V. V. Flambaum, and A. Derevianko, Single-ion nuclear clock for metrology at the 19th decimal place, Phys. Rev. Lett. **108**, 120802 (2012).

[39] H. W. T. Morgan, R. Elwell, J. E. S. Terhune, H. B. Tran Tan, U. C. Perera, A. Derevianko, A. N. Alexandrova, and E. R. Hudson, Proposal and theoretical investigation of ^{229}Th-doped nonlinear optical crystals for compact solid-state clocks, Appl. Phys. Lett. **126**, 111101 (2025).

[40] S. M. Girvin and L. Radzihovsky, Prospects for a solid-state nuclear clock, arXiv:2511.13017.

[41] T. Masuda, A. Yoshimi, A. Fujieda, H. Fujimoto, H. Haba, H. Hara, T. Hiraki, H. Kaino, Y. Kasamatsu, S. Kitao, K. Konashi, Y. Miyamoto, K. Okai, S. Okubo, N. Sasao, M. Seto, T. Schumm, Y. Shigekawa, K. Suzuki, S. Stellmer, *et al.*, X-ray pumping of the ^{229}Th nuclear clock isomer, Nature (London) **573**, 238 (2019).

[42] Q. Xiao, G. Penyazkov, R. Yu, B. Huang, J. Li, J. Shi, Y. Yu, Y. Mo, and S. Ding, Proposal for the generation of continuous-wave vacuum-ultraviolet laser light for Th-229 isomer precision spectroscopy, Phys. Rev. Appl. **25**, 024034 (2026).

[43] V. L. Ginzburg, On superconductivity and superfluidity (what I have and have not managed to do), as well as on the 'physical minimum' at the beginning of the XXI century (December 8, 2003), Phys.-Usp. **47**, 1155 (2004).

[44] E. V. Tkalya, Proposal for a nuclear gamma-ray laser of optical range, Phys. Rev. Lett. **106**, 162501 (2011).

[45] E. V. Tkalya, C. Schneider, J. Jeet, and E. R. Hudson, Radiative lifetime and energy of the low-energy isomeric level in ^{229}Th, Phys. Rev. C **92**, 054324 (2015).

[46] Y. Wang, Y. Yang, Y. Li, D. Yue, K. Zhao, Y. Wang, C. Fu, and Y. Ma, Enhanced yield rate of ^{229m}Th via cascade decay in storage rings and electron beam ion traps, Phys. Rev. C **113**, 054602 (2026).

[47] F. Schaden, T. Riebner, I. Morawetz, L. T. De Col, G. A. Kazakov, K. Beeks, T. Sikorsky, T. Schumm, K. Zhang, V. Lal, G. Zitzer, J. Tiedau, M. V. Okhapkin, and E. Peik, Laser-induced quenching of the Th-229 nuclear clock isomer in calcium fluoride, Phys. Rev. Res. **7**, L022036 (2025).

[48] C. Zhang, T. Ooi, J. S. Higgins, J. F. Doyle, L. von der Wense, K. Beeks, A. Leitner, G. A. Kazakov, P. Li, P. G. Thirolf, T. Schumm, and J. Ye, Frequency ratio of the ^{229m}Th nuclear isomeric transition and the ^{87}Sr atomic clock, Nature (London) **633**, 63 (2024).

[49] R. Elwell, C. Schneider, J. Jeet, J. E. S. Terhune, H. W. T. Morgan, A. N. Alexandrova, H. B. Tran Tan, A. Derevianko, and E. R. Hudson, Laser excitation of the ^{229}Th nuclear isomeric transition in a solid-state host, Phys. Rev. Lett. **133**, 013201 (2024).

[50] N. Minkov and A. Pálffy, Reduced transition probabilities for the gamma decay of the 7.8 eV isomer in ^{229}Th, Phys. Rev. Lett. **118**, 212501 (2017).

[51] A. M. Dykhne and E. V. Tkalya, Matrix element of the anomalously low-energy (3.5 ± 0.5 eV) transition in ^{229}Th and the isomer lifetime, J. Exp. Theor. Phys. Lett. **67**, 251 (1998).

[52] N. Minkov and A. Pálffy, Theoretical predictions for the magnetic dipole moment of ^{229m}Th, Phys. Rev. Lett. **122**, 162502 (2019).

[53] N. Minkov and A. Pálffy, ^{229m}Th isomer from a nuclear model perspective, Phys. Rev. C **103**, 014313 (2021).

[54] Z.-R. Chen, L.-J. Wang, and Y. Wu, Microscopic nuclear structure study of ^{229}Th by projected shell model, Phys. Lett. B **869**, 139858 (2025).

[55] E. F. Zhou and J. M. Yao, Microscopic study of low-lying states in odd-mass nuclei for atomic electric dipole moment searches, arXiv:2511.05984.

[56] N. Minkov, A. Pálffy, P. Quentin, and L. Bonneau, Skyrme-Hartree-Fock-BCS approach to ^{229m}Th and neighboring nuclei, Phys. Rev. C **110**, 034327 (2024).

[57] P. L. Sassarini, J. Dobaczewski, J. Bonnard, and R. F. Garcia Ruiz, Nuclear DFT analysis of electromagnetic moments in odd

near doubly magic nuclei, J. Phys. G: Nucl. Part. Phys. **49**, 11LT01 (2022).
[58] J. Bonnard, J. Dobaczewski, G. Danneaux, and M. Kortelainen, Nuclear DFT electromagnetic moments in heavy deformed open-shell odd nuclei, Phys. Lett. B **843**, 138014 (2023).
[59] H. Wibowo, B. C. Backes, J. Dobaczewski, R. P. de Groote, A. Nagpal, A. Sánchez-Fernández, X. Sun, and J. L. Wood, Electromagnetic moments in the Sn-Gd region determined within nuclear DFT, J. Phys. G: Nucl. Part. Phys. **52**, 065104 (2025).
[60] J. Dobaczewski, A. E. Stuchbery, G. Danneaux, A. Nagpal, P. L. Sassarini, and H. Wibowo, Electromagnetic moments of ground and excited states calculated in heavy odd-N open-shell nuclei, Phys. Rev. C **113**, 024306 (2026); **113** 044312 (2026).
[61] J. Dobaczewski, B. Backes, R. de Groote, A. Restrepo-Giraldo, X. Sun, and H. Wibowo, Electromagnetic and exotic moments in nuclear density functional theory, Ann. Rev. Nucl. Part. Sci. **76**, 459 (2026).
[62] J. Miśkiewicz, M. Konieczka, and W. Satuła, Two-neutrino $0^+ \to 0^+$ double-β decay of ^{48}Ca within the density-functional-theory–based no-core configuration-interaction framework, Phys. Rev. C **112**, 055502 (2025).
[63] J. Dobaczewski, P. Bączyk, P. Becker, M. Bender, K. Bennaceur, J. Bonnard, Y. Gao, A. Idini, M. Konieczka, M. Kortelainen, L. Próchniak, A. M. Romero, W. Satuła, Y. Shi, L. F. Yu, and T. R. Werner, Solution of universal nonrelativistic nuclear DFT equations in the Cartesian deformed harmonic-oscillator basis. (IX) HFODD (v3.06h): A new version of the program, J. Phys. G: Nucl. Part. Phys. **48**, 102001 (2021).
[64] J. Dobaczewski *et al.*, Code HFODD, version to be published, 2026.
[65] A. Restrepo-Giraldo *et al.*, Code HFODD, the user's guide, to be published, 2026.
[66] See Supplemental Material at http://link.aps.org/supplemental/10.1103/khzg-vkgr for the lists of nonconverged and/or singular points, parameters and numerical conditions of the calculation, results presented in numerical form, and plots of electromagnetic moments calculated in this Letter, which includes Refs. [87,94].
[67] M. Bender, J. Dobaczewski, J. Engel, and W. Nazarewicz, Gamow-Teller strength and the spin-isospin coupling constants of the Skyrme energy functional, Phys. Rev. C **65**, 054322 (2002).
[68] B. A. Brown, New skyrme interaction for normal and exotic nuclei, Phys. Rev. C **58**, 220 (1998).
[69] J. Bartel, P. Quentin, M. Brack, C. Guet, and H.-B. Håkansson, Towards a better parametrisation of Skyrme-like effective forces: A critical study of the SkM force, Nucl. Phys. A **386**, 79 (1982).
[70] M. Kortelainen, T. Lesinski, J. Moré, W. Nazarewicz, J. Sarich, N. Schunck, M. V. Stoitsov, and S. Wild, Nuclear energy density optimization, Phys. Rev. C **82**, 024313 (2010).
[71] M. Beiner, H. Flocard, N. V. Giai, and P. Quentin, Nuclear ground-state properties and self-consistent calculations with the Skyrme interaction: (I). Spherical description, Nucl. Phys. A **238**, 29 (1975).
[72] P.-G. Reinhard, Skyrme forces and giant resonances in exotic nuclei, Nucl. Phys. A **649**, 305 (1999).
[73] E. Chabanat, P. Bonche, P. Haensel, J. Meyer, and R. Schaeffer, A Skyrme parametrization from subnuclear to neutron star densities Part II. Nuclei far from stabilities, Nucl. Phys. A **635**, 231 (1998).
[74] M. Kortelainen, J. McDonnell, W. Nazarewicz, P.-G. Reinhard, J. Sarich, N. Schunck, M. V. Stoitsov, and S. M. Wild, Nuclear energy density optimization: Large deformations, Phys. Rev. C **85**, 024304 (2012).
[75] J. Dobaczewski, J. Engel, M. Kortelainen, and P. Becker, Correlating Schiff moments in the light actinides with octupole moments, Phys. Rev. Lett. **121**, 232501 (2018).
[76] L. P. Gaffney, P. A. Butler, M. Scheck, A. B. Hayes, F. Wenander, M. Albers, B. Bastin, C. Bauer, A. Blazhev, S. Bönig, N. Bree, J. Cederkäll, T. Chupp, D. Cline, T. E. Cocolios, T. Davinson, H. De Witte, J. Diriken, T. Grahn, A. Herzan, *et al.*, Studies of pear-shaped nuclei using accelerated radioactive beams, Nature (London) **497**, 199 (2013).
[77] H. J. Wollersheim, H. Emling, H. Grein, R. Kulessa, R. S. Simon, C. Fleischmann, J. de Boer, E. Hauber, C. Lauterbach, C. Schandera, P. A. Butler, and T. Czosnyka, Coulomb excitation of ^{226}Ra, Nucl. Phys. A **556**, 261 (1993).
[78] F. K. McGowan, C. E. Bemis, W. T. Milner, J. L. C. Ford, R. L. Robinson, and P. H. Stelson, Coulomb excitation of vibrational-like states in the even-A actinide nuclei, Phys. Rev. C **10**, 1146 (1974).
[79] Y. M. Engel, D. M. Brink, K. Goeke, S. J. Krieger, and D. Vautherin, Time-dependent Hartree-Fock theory with Skyrme's interaction, Nucl. Phys. A **249**, 215 (1975).
[80] E. Perlińska, S. G. Rohoziński, J. Dobaczewski, and W. Nazarewicz, Local density approximation for proton-neutron pairing correlations: Formalism, Phys. Rev. C **69**, 014316 (2004).
[81] N. Schunck, *Energy Density Functional Methods for Atomic Nuclei*, IOP Expanding Physics (IOP, Bristol, England, 2019).
[82] L. Bonneau, N. Minkov, D. D. Duc, P. Quentin, and J. Bartel, Effect of core polarization on magnetic dipole moments in deformed odd-mass nuclei, Phys. Rev. C **91**, 054307 (2015).
[83] A. Idini, K. Bennaceur, and J. Dobaczewski, Landau parameters for energy density functionals generated by local finite-range pseudopotentials, J. Phys. G: Nucl. Part. Phys. **44**, 064004 (2017).
[84] P. Ring and P. Schuck, *The Nuclear Many-Body Problem* (Springer-Verlag, Berlin, 1980).
[85] J. Dobaczewski, W. Satuła, B. Carlsson, J. Engel, P. Olbratowski, P. Powałowski, M. Sadziak, J. Sarich, N. Schunck, A. Staszczak, M. Stoitsov, M. Zalewski, and H. Zduńczuk, Solution of the Skyrme-Hartree-Fock-Bogolyubov equations in the Cartesian deformed harmonic-oscillator basis.: (VI) HFODD (v2.40h): A new version of the program, Comput. Phys. Commun. **180**, 2361 (2009).
[86] G. Bertsch, J. Dobaczewski, W. Nazarewicz, and J. Pei, Hartree-Fock-Bogoliubov theory of polarized Fermi systems, Phys. Rev. A **79**, 043602 (2009).
[87] J. Dobaczewski and J. Dudek, Solution of the Skyrme-Hartree-Fock equations in the Cartesian deformed harmonic oscillator basis II. The program HFODD, Comput. Phys. Commun. **102**, 183 (1997).
[88] J. A. Sheikh, J. Dobaczewski, P. Ring, L. M. Robledo, and C. Yannouleas, Symmetry restoration in mean-field approaches, J. Phys. G: Nucl. Part. Phys. **48**, 123001 (2021).
[89] J. Sadoudi, M. Bender, K. Bennaceur, D. Davesne, R. Jodon, and T. Duguet, Skyrme pseudo-potential-based EDF parametrization for spuriousity-free MR EDF calculations, Phys. Scr., T **154**, 014013 (2013).

[90] J. Sadoudi, T. Duguet, J. Meyer, and M. Bender, Skyrme functional from a three-body pseudopotential of second order in gradients: Formalism for central terms, Phys. Rev. C **88**, 064326 (2013).

[91] K. Bennaceur, A. Idini, J. Dobaczewski, P. Dobaczewski, M. Kortelainen, and F. Raimondi, Nonlocal energy density functionals for pairing and beyond-mean-field calculations, J. Phys. G: Nucl. Part. Phys. **44**, 045106 (2017).

[92] P. Klüpfel, P.-G. Reinhard, T. J. Bürvenich, and J. A. Maruhn, Variations on a theme by Skyrme: A systematic study of adjustments of model parameters, Phys. Rev. C **79**, 034310 (2009).

[93] Repository of raw data obtained in this work is available at https://webfiles.york.ac.uk/HFODD/Projects/229Th.

[94] J. C. Slater, A simplification of the Hartree-Fock method, Phys. Rev. **81**, 385 (1951).